Supplement of Atmos. Chem. Phys., 21, 393–413, 2021
https://doi.org/10.5194/acp-21-393-2021-supplement

Atmospheric Chemistry and Physics
Open Access
EGU

Supplement of

Measurement report: Changing characteristics of atmospheric CH_4 in the Tibetan Plateau: records from 1994 to 2019 at the Mount Waliguan station

Shuo Liu et al.

Correspondence to: Shuangxi Fang (fangsx@cma.gov.cn) and Zhaozhong Feng (zhzhfeng201@hotmail.com)

Table S1. The diurnal peak to trough amplitude over different observing periods during 1994-2019 at the WLG station.

	1994-1997	1998-2002	2003-2007	2008-2012	2013-2019	1994-2019
Spring	6.5 ± 3.1	4.7 ± 2.1	5.6 ± 2.7	7.0 ± 3.1	6.9 ± 3.1	5.8 ± 2.8
Summer	5.6 ± 3.9	4.4 ± 3.3	4.7 ± 2.4	6.5 ± 3.1	5.5 ± 3.4	4.4 ± 3.4
Autumn	4.7 ± 3.9	5.7 ± 4.0	4.2 ± 2.5	7.1 ± 3.5	4.8 ± 3.1	4.3 ± 3.1
Winter	12.5 ± 3.6	9.7 ± 4.8	5.9 ± 2.8	7.5 ± 4.1	9.2 ± 3.6	7.1 ± 2.9

Table S2. The seasonal averages of atmospheric CH_4 in the City Regions (CR), the Tibet Plateau (TP), and the total regional records during 1994-2019 at the WLG station.

		1994-1997	1998-2002	2003-2007	2008-2012	2013-2019	1994-2019
Spring	CR	1807.3 ± 0.2	1813.5 ± 0.3	1830.4 ± 0.2	1863.9 ± 0.3	1906.2 ± 0.3	1852.2 ± 0.4
	TP	1804.4 ± 0.2	1822.2 ± 0.2	1829.5 ± 0.3	1864.0 ± 0.3	1905.0 ± 0.2	1853.1 ± 0.3
	Total	1807.3 ± 0.2	1822.9 ± 0.2	1829.4 ± 0.3	1858.0 ± 0.3	1907.7 ± 0.2	1853.1 ± 0.3
Summer	CR	1809.6 ± 0.2	1828.4 ± 0.3	1840.0 ± 0.2	1871.4 ± 0.2	1921.9 ± 0.3	1862.4 ± 0.4
	TP	1807.3 ± 0.2	1833.1 ± 0.2	1840.1 ± 0.2	1870.8 ± 0.3	1919.4 ± 0.3	1862.8 ± 0.4
	Total	1807.8 ± 0.2	1833.1 ± 0.2	1839.3 ± 0.2	1865.5 ± 0.2	1920.5 ± 0.3	1861.7 ± 0.4
Autumn	CR	1800.4 ± 0.2	1825.9 ± 0.4	1841.8 ± 0.2	1862.0 ± 0.2	1908.3 ± 0.4	1852.0 ± 0.3
	TP	1800.8 ± 0.2	1831.4 ± 0.4	1842.8 ± 0.3	1861.4 ± 0.2	1907.3 ± 0.3	1853.0 ± 0.3
	Total	1800.6 ± 0.2	1831.3 ± 0.4	1842.6 ± 0.3	1860.2 ± 0.2	1911.7 ± 0.4	1855.9 ± 0.4
Winter	CR	1818.9 ± 0.3	1823.7 ± 0.4	1840.3 ± 0.2	1869.2 ± 0.3	1910.1 ± 0.3	1858.5 ± 0.3
	TP	1809.0 ± 0.1	1831.4 ± 0.4	1838.1 ± 0.2	1863.0 ± 0.3	1903.7 ± 0.3	1855.3 ± 0.3
	Total	1813.3 ± 0.2	1830.4 ± 0.3	1837.3 ± 0.2	1860.7 ± 0.3	1907.2 ± 0.3	1856.7 ± 0.3

Table S3. The statistics of the excluding trajectories over different observing periods during 2004-2017 at the WLG station.

		Jan	Feb	Mar	Apr	May	Jun	Jul	Aug	Sep	Oct	Nov	Dec	Sum
2005-2007	Total	764	1193	938	1190	882	1139	921	1431	1427	843	1272	911	12911
	Reject	157	111	51	371	545	767	632	1325	911	181	133	19	5203
2008-2012	Total	3060	2081	1764	1811	1136	2250	1919	2826	2791	1527	1868	1079	24112
	Reject	41	228	194	467	675	1681	1428	1727	1298	90	0	0	7829
2013-2017	Total	2110	1738	2112	1882	1269	1259	461	1816	2186	1659	1844	1111	19447
	Reject	0	1	0	55	81	0	90	875	138	71	0	12	1323

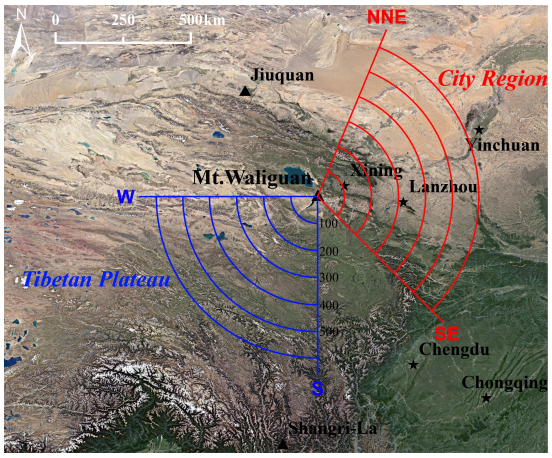

Figure S1. The geographical distribution of the two CH_4 source regions, including the City Regions covered from the northeast and southeast (NNE-…SE) of the WLG and the Tibetan Plateau located south to west (S-…-W) of the station. The remote sensing image layer was downloaded from© Google Earth.

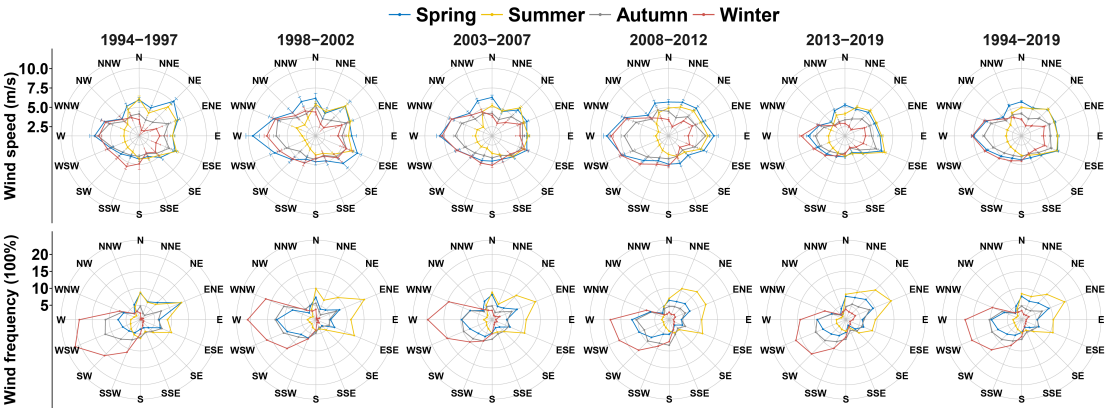

Figure S2. The wind-rose distribution of wind frequency and wind speed from 16 horizontal wind directions over different periods during 1994-2019 at the WLG station. The different colors represent the CH_4 data in different seasons. Error bars of the wind speed indicate 95% confidence intervals.

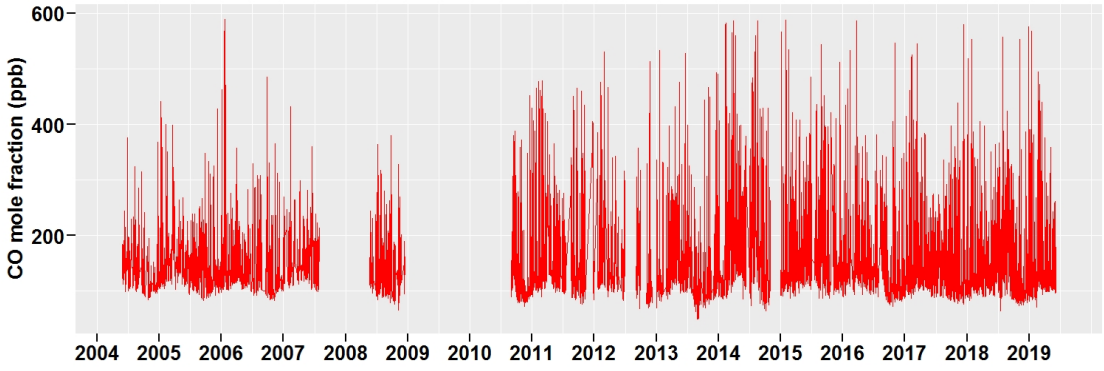

Figure S3. The hourly CO data from 2004 to 2019 at the WLG station.

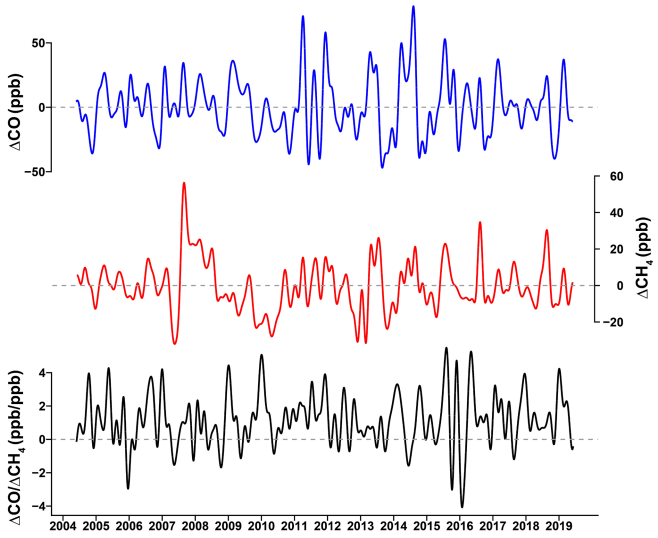

Figure S4. The time series of ΔCO, ΔCH_4 and $\Delta CO/\Delta CH_4$ from 2004 to 2019 at the WLG station.

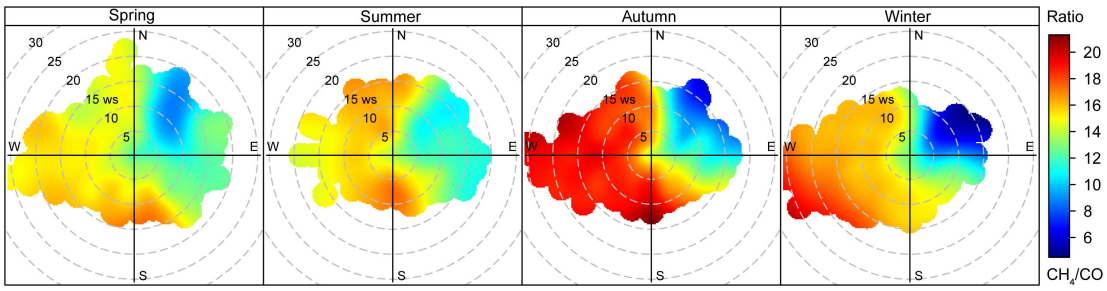

Figure S5. The seasonal polar plot of CH_4/CO ratio during 2004-2019 at the WLG station. The gradient colors represent the level of ratio values.

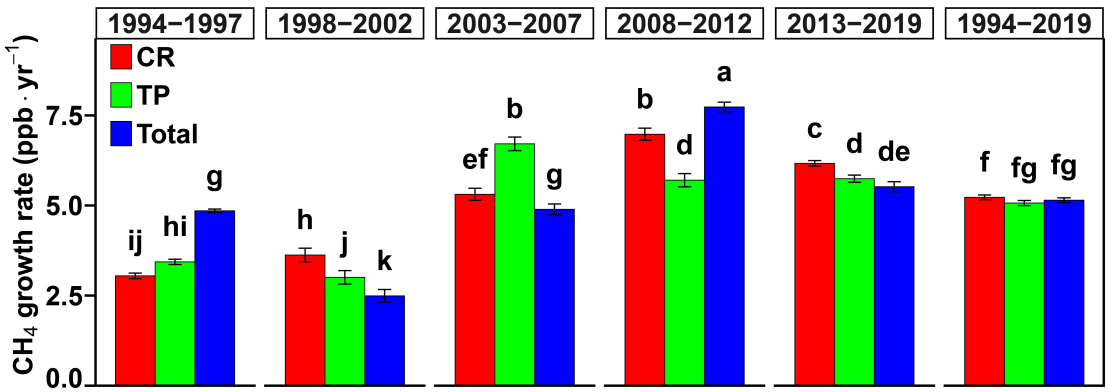

Figure S6. The annual growth rates of atmospheric CH_4 over different observing periods in 1994-2019 at the WLG station. The 'CR', 'TP', and 'Total' respectively represent the measurements from the City Regions, the Tibet Plateau, and the total regional records. Different letters represent the significant difference between regions and periods.

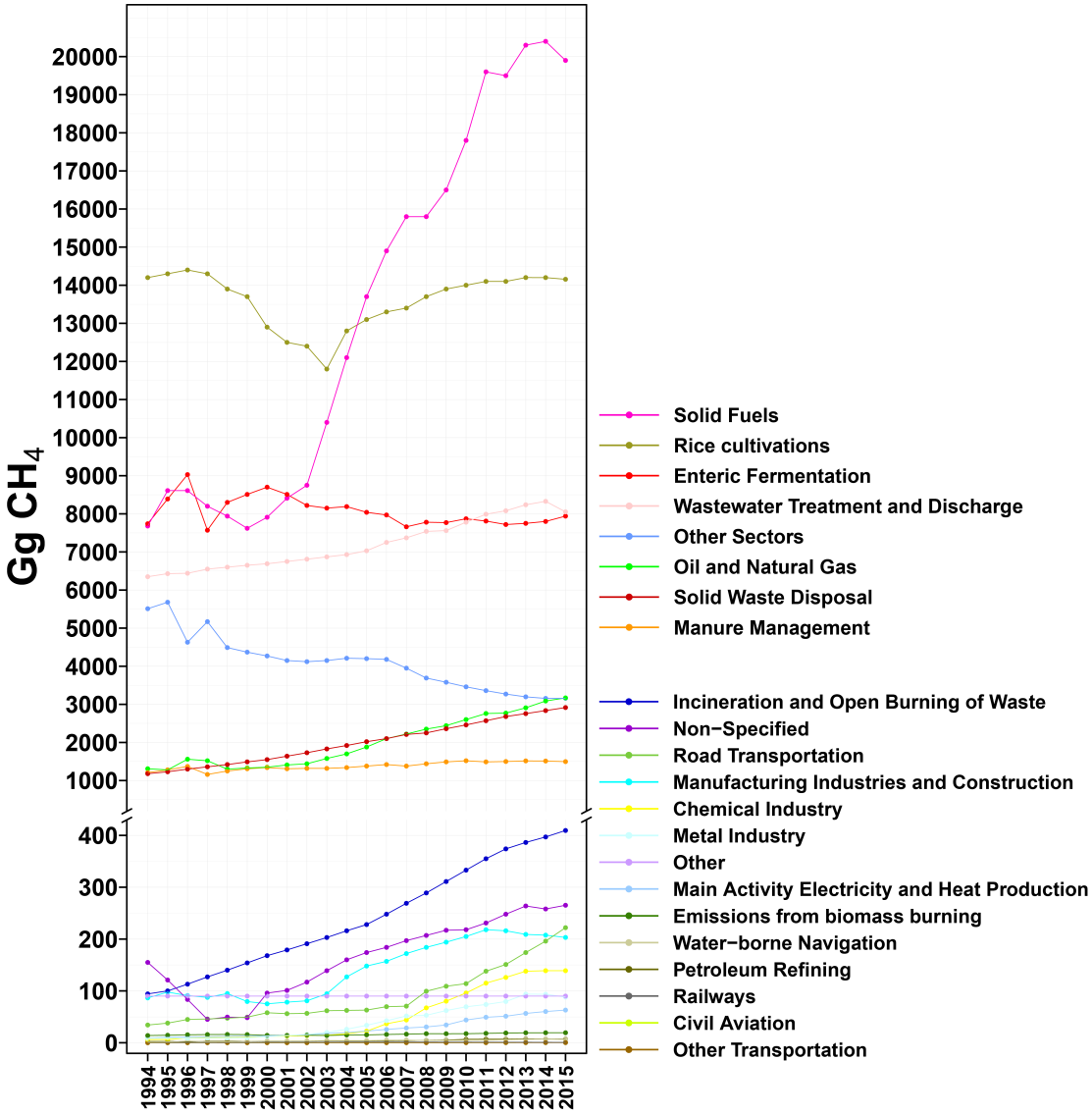

Figure S7. The CH_4 emissions per sector in China over 1994-2015 based on Emissions Database for Global Atmospheric Research (EDGAR).

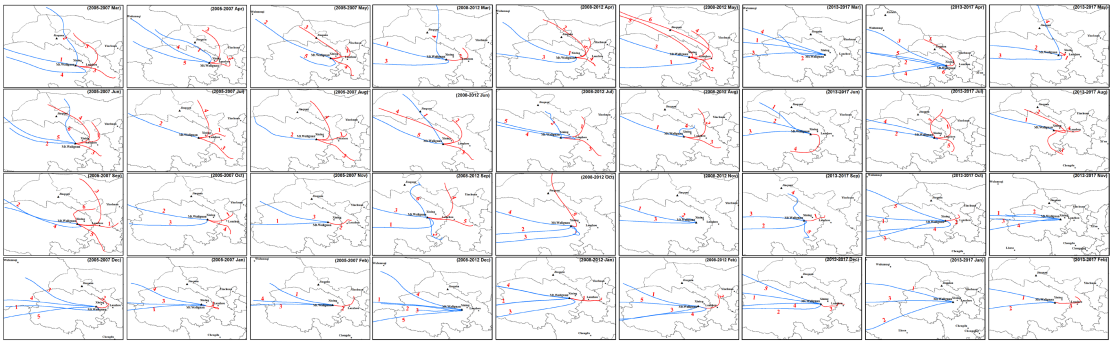

Figure S8. The monthly cluster analysis of hourly trajectories during 2005-2017 at the WLG station. The red clusters represent air masses transport from city regions.

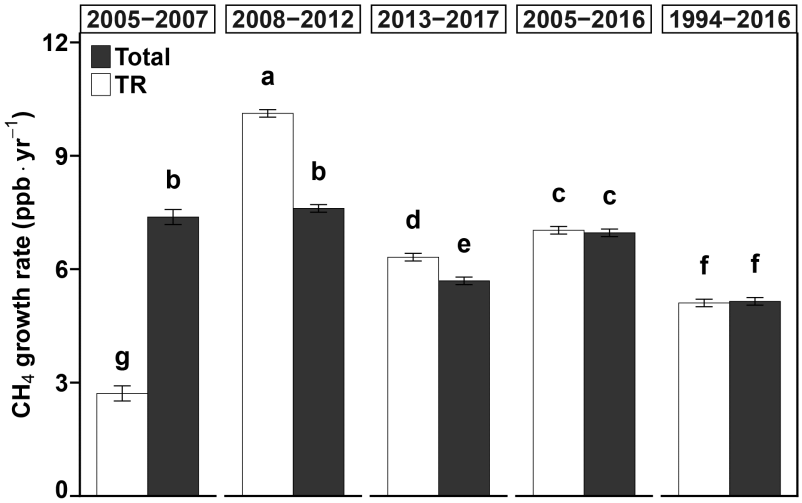

Figure S9. The annual growth rates of atmospheric CH_4 over different periods during 2005-2017 at the WLG station. 'TR' refers to the growth rate of the regional data that without air mass transport from city regions. 'Total' refers to the growth rate of original regional data series. Different letters represent significant differences among the cases.

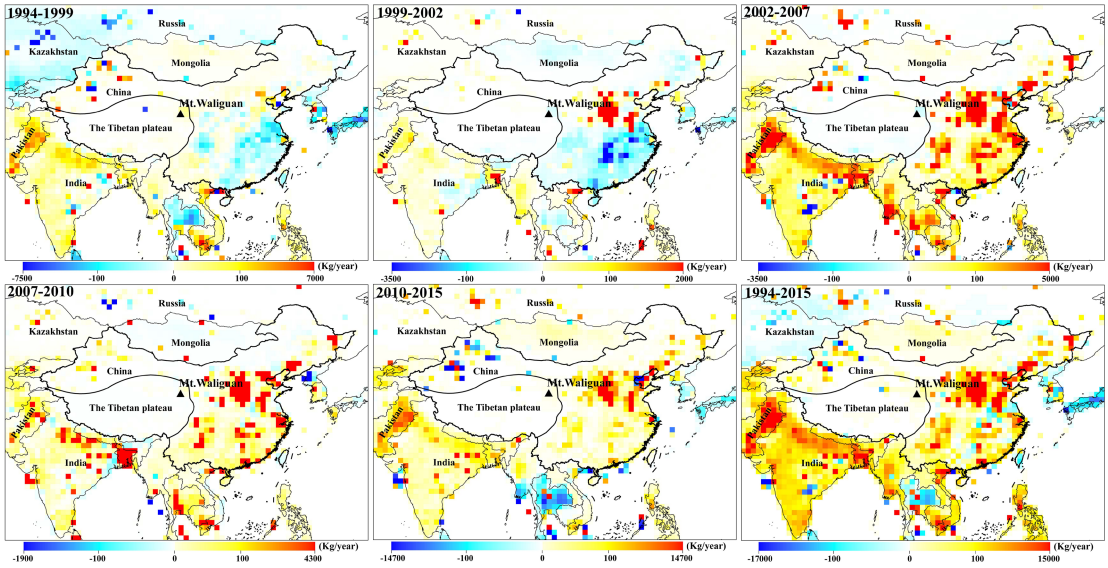

Figure S10. The geographical distribution of the CH_4 emission increase in different periods during 1994-2015, based on the data from Emissions Database for Global Atmospheric Research (EDGAR).